Case Reports in Ophthalmology

Case Rep Ophthalmol 2017;8:545–557

DOI: 10.1159/000485316
Published online: December 14, 2017

Case Report

Application of Arterial Spin Labelling in Detecting Retinal Ischemia

Ehsan Vaghefi[a, b] Kevin Kauv[a] Wilson Pan[a] David Squirrell[a, c]

[a]School of Optometry and Vision Science, University of Auckland, Auckland, New Zealand;
[b]Auckland Bioengineering Institute, University of Auckland, Auckland, New Zealand;
[c]Auckland District Health Board Ophthalmology Services, Auckland, New Zealand

Keywords
Chorioretinal blood flow · Chorioretinal ischemia · Arterial spin labelling

Abstract
Purpose: Here, we have tried to quantify the chorioretinal blood perfusion in patients who are clinically identified to be suffering from retinal ischemia using arterial spin labelling (ASL) MRI. ***Method:*** Four participants, diagnosed with retinal ischemia based on their structural OCT and angiography test, were then scanned using anatomical MRI as well as ASL. We optimized MR parameters to maximize resolution and target fixation, blinking, and breathing ques to minimize motion artifacts. ***Results:*** Participants had a maximum of ~50 mL/100 mL/min of blood perfusion, which is below the normal values of ~200 mL/100 mL/min. It also appeared that thinning of the choroid contributes more to the measured decreased chorioretinal perfusion, compared to slowed arterial filling time. ***Conclusion:*** Decreased chorioretinal perfusion is a multifactorial event and has been implicated in several posterior eye pathologies. Based on our current results, it seems that ischemia of the eye could be due to anatomy (tissue volume) and/or functionality (arterial flow).

KARGER

Dr. Ehsan Vaghefi
School of Optometry and Vision Science, University of Auckland
85 Park Rd, Grafton
Auckland 1023 (New Zealand)
E-Mail e.vaghefi@auckland.ac.nz

Introduction

Our sense of vision is the product of accurate functioning of numerous elements comprising the optical pathway of our eyes. The anterior part of the human eye consists of the cornea, lens, ciliary muscles, and zonule fibers. Coordinated operation of these structures projects a clear image onto the retina, located at the back of the eye. By way of a complex sequence of neural encoding, the retina then converts the light signals into a set of neuro-electrical signals that are transferred to the brain via the optic nerve for further processing and perception. Anatomically, the retina consists of multiple cell types organized into layers, functionally performing different processing tasks [1]. Distinct and yet interdependent functions of each of these cell layers create and support the photo-transduction process [1].

The human retina requires a rich blood supply due to its high metabolic demand, especially of the retinal pigment epithelium and the photoreceptors of the outer retina. The average central thickness of the retina and choroid are 209.1 ± 12.9 μm and 292.7 ± 77.3 μm, respectively [2]. The retina consists of 2 arterial systems, the retinal vasculature and the choroidal vasculature, both of which are supplied by the branches of the ophthalmic artery, which itself is a branch of the internal carotid artery [3]. The choroid is an extremely vascular tissue comprised of a dense plexus of fenestrated capillaries, which are mainly supplied by the posterior ciliary arteries, but involve some branches of the anterior ciliary arteries [4].

The central retinal artery is the origin of the retinal vascular bed, which in turn supplies the inner two-thirds of the retina. The outer retina and fovea are avascular and thus rely instead on the choroidal circulation and choriocapillaris for nourishment and oxygen supply. Previous studies have suggested that inner retinal vasculature has been fine-tuned to give sufficient blood flow supply with minimal light blockage, and thus there is a very little margin of error for retinal perfusion [5–7]. Therefore, pathologies resulting in vasculature disruption or non-perfusion have significant adverse consequences on the health of the retina and quality of overall vision [2, 8].

Ischemia is a term that describes the hypo-perfusion or "restrained blood supply" of the tissue, resulting in a reduction of the supply of nutrients, as well as the drainage of waste [8]. If left untreated, chorioretinal ischemia can result in profound irreversible loss of vision. Ischemia of the retinal and/or choroidal vasculature is seen in conditions such as diabetic retinopathy, retinal artery or vein occlusions, age-related macular degeneration (AMD), retinopathy of prematurity, ocular ischemic syndrome, and severe myopia. These conditions are generally multifactorial, initially involving disruption of the chorioretinal blood supply or vaso-obliteration/microvascular degeneration [5, 9]. As the ischemia progresses, hypo-perfusion of the retina and choroid can trigger a vaso-proliferative phase, in which pro-angiogenic factors are released [9, 10], such as vascular endothelial growth factor (VEGF) [7]. This results in neovascularization in the retina, which is associated with increased leakages, macular edema, fibro-vascular scar formation [10], hemorrhages, and rubeosis iridis if severe [11]. Therefore, early diagnosis of chorioretinal ischemia and blood hypo-perfusion is paramount for initiating intervention and management of these pathologies.

Currently, there are very few techniques capable of detecting and monitoring chorioretinal ischemia. These include ophthalmoscopy, fluorescein and indocyanine-green angiography, optical coherence tomography angiography (OCT-A), and magnetic resonance im-

aging (MRI) when used in arterial spin labelling (ASL) mode [12]. In traditional angiography, auto-fluorescent molecules are injected into the blood stream, and as the blood column containing the dye enters the eye, the reagent is exposed to predetermined light wavelengths, which results in the hyper-fluorescence of the reagent-enhanced blood vessels. They can provide structural information on the chorioretinal vasculature, areas of normal perfusion, reduced perfusion, or leakage; this is a snapshot of the current state. Although widely used, the utility of the traditional angiographic techniques is limited by the fact that they only reveal a snapshot of the current state of the tissue [13]. Measuring the time taken for the dye-laden blood column to enter the retinal circulation via dynamic high-speed angiography can give additional insights into the perfusion of the chorioretinal circulations, being delayed in cases where there is reduced perfusion pressure, most often due to an obstruction or stenosis within the arterial tree proximal to the globe [14].

The recently introduced modality of OCT-A is capable of structural and functional retinal imaging. The OCT-A functional blood flow signal is based on speckle noise generated by a moving particle (i.e., blood cells) in the field of view (i.e., retinal arteries) [15]. Compared to fluorescein and indocyanine-green angiography, OCT-A is non-invasive and potentially 3D [16, 17]. Current OCT-A can generate volumetric blood flow datasets in seconds [18]. However, OCT-A also has shortcomings. Firstly, only a snapshot of retinal blood flow can be obtained. Second, OCT-A is unable to image any potential leakages of chorioretinal vasculature [19]. Moreover, while OCT-A is capable of imaging both retinal and choroidal arteries, the larger retinal vessels often block the view of choroidal arteries, which can lead to misdiagnosis of outer retinal vascular abnormalities and could also miss areas of slow blood flow in micro-aneurysms, polypoidal lesions, or fibrotic choroidal neovascularization [18]. Finally and critically, OCT-A is only qualitative and cannot quantify chorioretinal blood flow.

MRI in ASL mode, on the other hand, is a relatively new technique that can non-invasively provide high-resolution quantitative measures of blood flow, and has been mainly utilized for brain imaging. ASL, once analyzed, can measure the perfusion of blood in units of mL/100 mL/min [20]. Thus, when applied to the eye, it would allow for measurement of blood perfusion in the back of the eye, highlighting any potential areas of hypo-perfusion and aid in understanding of the factors affecting the chorioretinal blood flow and its changes due to chorioretinal ischemia. ASL modality and its optimum parameters for ocular implementation have been reviewed in depth elsewhere [20], but in short, it starts by magnetically tagging the water in arterial blood, using radio-frequency pulses prior to entering the tissue of interest. The next step is to record the signal from the tagged molecules as they arrive at the region of interest. This labelled scan is then compared to a control scan without any tagging, which is performed at a delay [21]. The amount of labelled (tagged) arterial blood, transferred from the arteries to the tissue of interest, is found via the difference between the labelled scan and the control scan [22, 23]. The feasibility of the use of ASL in the healthy eye has been investigated previously in the literature [12].

The aim of this pilot study was to investigate the potential utility of ASL as a non-invasive quantitative technique to study the hemodynamic changes in the retinal and choroidal vasculature in a small cohort of individuals with ocular disease, who would be expected to have reduced chorioretinal perfusion from their clinical appearances, angiographic characteristics, and OCT findings. As such, this study represents for the first time that the technique

of ASL has been used to measure localized chorioretinal perfusion in eyes of individuals who have ocular pathology.

Methods

Subject Recruitment

Four participants who were, on the basis of clinical findings, expected to have either reduced choroidal or retinal perfusion or both were recruited in this study, which was approved by the University of Auckland Human Participants Ethics Committee. These participants were identified based on their clinical findings on ophthalmoscopy, the status of the retinal capillary bed and arterial filling time on fluorescein angiography, and their subfoveal choroidal thickness (Table 1). The participants were aged between 56 and 83 years and included 2 males and 2 females. Two individuals had profound ocular ischemia, 1 individual had pathological myopia and a thin choroid, and 1 individual had a thin choroid and dry AMD with evidence of reticular pseudo-drusen with no associated atrophy.

The participants did not have any known MRI contraindications, and exclusion criteria included family history of epilepsy or seizures, history of neurological disorders or disease, presence of a cardiac pacemaker or other metal implants, serious head injuries, or pregnancy. Participants were imaged on a single session, which included T1-weighted and T2-weighted anatomical scans of the eyes and brain (about 4 min long), followed by ASL scans of each eye (about 7 min per eye), totalling about 30 min per session. Participants were instructed to fixate on a cross-target that was projected inside the MRI room and take calm relaxed breaths as eye movements and movements of the eye coil cords resting on their chest could result in motion artefacts in the images.

Angiography

All participants underwent fluorescein angiography, utilizing established protocols, within 4 weeks of their MRI ASL assessment. In all cases, 5 mL of 20% sodium fluorescein was injected into the antecubital fossa via a 23-G cannula. The arterial filling time was defined as the time taken from administration of the dye to its first appearance within the retinal arterial system. The timer was started when the physician started injecting the bolus of fluorescein into the cannula. A single physician conducted all the angiograms in this study. As this is a dynamic measurement, it was only possible to determine the dye transit time to 1 eye per angiographic assessment. Clinical need determined that participant number 2 2 two separate fluorescein angiograms to assess their profound ocular ischemia and thus the arterial filling times for both eyes were known. In the other 3 participants, the fluorescein angiogram was only performed once, and thus we only have accurate filling data for 1 eye.

Choroidal OCT

Central macular thickness was assessed using the Heidelberg Spectralis OCT on the single-line scan choroidal enhanced-depth imaging (EDI) mode. The central macular choroidal thickness was measured manually and was taken to be the distance between calipers placed on the Bruch's membrane and the sclera under the fovea.

MRI Acquisition

Participants were scanned using the 3T MAGNETOM SKYRA clinical MRI (Siemens, Germany) at the Centre for Advanced MRI at the University of Auckland. A 20-channel head coil was used as the transmitter, in conjunction with an additional specialized eye coil (4 cm in diameter), to enhance the received signal. Both coils were supplied by Siemens Health Care. A customized soft mask was padded under the eye coil, to minimize the direct contact between tissue and coils. During the MRI acquisition, participants were guided to focus on a fixation target that was projected inside the MRI room. This led to minimized eye movements and hence motion artefact of the outcome. The participants were guided to rest their eyes in between each imaging sequence.

The imaging protocols in this study included a 3D T1-weighted anatomical imaging, plus a 3D ASL imaging with pCASL technique. The structural images were acquired with a magnetization-prepared rapid gradient-echo (MP-RAGE) sequence [22, 24]. The imaging parameters were TE = 2.13 ms, TR = 1,900 ms, isometric voxel size = 0.9 × 0.9 × 0.9 m, slices = 176, parallel imaging mode: GRAPPA, acceleration factor: 2.

The ASL images were acquired subsequently. To acquire the labelled images, a tagging plane was located at 7 cm below the optical nerve. This has proven to be the optimal location to label the retinal blood flow from previous investigations [12, 25]. The labelling duration was 1,500 ms and the post-labelling duration was 1,500 ms. The labelling pulse was then turned off to acquire the control image. The readout sequence used in our pCASL was a turbo-gradient spin echo with the following parameters: TR = 5,000 ms, TE = 26.52 ms, FOV = 130 × 130 mm, matrix size = 128 × 128 (in-plane resolution of 0.8 × 0.8 mm), slice thickness = 3 mm, bandwidth = 1,502 Hz/Px, turbo-factor = 14, EPI factor = 21. The image acquisitions alternated between control and label, and a total of 6 control-label pairs were acquired for each eye. Apart from the control and label sets, a reference image (M0) was acquired prior to the control-label series. The M0 image has the same imaging parameters mentioned above, but without labelling preparations. The time duration for the ASL for 1 eye is about 7 min and 30 s, and the overall imaging session took about 30 min to complete.

Post-Processing

The acquired control and label images were first reviewed manually and images subject to significant motion artefacts were discarded. Next, the stack of control and label images were per-processed using the SPM package (www.fil.ion.ucl.ac.uk/spm/) based on the Matlab platform (MathWorks Inc., Natick, MA, USA). The images were then smoothed by a Gaussian kernel (FWHM = 5 mm). After that, the stack of control and label images was spatially realigned to the reference image (M0). The realignment was performed with a rigid body spatial transformation, in which the points were sampled at 4 mm distance apart from the M0 image and with 4th order B-spline interpolation during re-sampling (Fig. 1) [26]. The alignment of labelled-control image pairs maximized the ASL (Fig. 2).

To calculate the retinal blood flows, only the slices were chosen where optical nerve and other orbital tissues were clearly apparent. Once the slice image was selected, the voxel-wise blood flow was calculated by the following equation proposed by Wang et al. [27]:

$$f = (2M_0a)/(\lambda R_{1a}\,\Delta M_{asl})\,[e^{(-wR_{1a})} - e^{-(\tau+w)\,R_{1a}}] \times 6{,}000.$$

where ΔM_{asl} is the average signal difference between control and label images, M_0 is the signal intensity of vitreous measured from the M_0 image [25], τ is the labelling time, w is the

post-labelling delay, R_{1a} is the reciprocal of longitudinal relaxation time of blood – measured as 0.67 s^{-1} at 3T [22], λ is the blood/tissue water partition coefficient, and a is the labelling efficiency. We assumed λ = 0.9 g/mL and a = 0.85. A factor of 6,000 was required to convert the blood flow into a physiological unit (mL/100 g/min).

Results

The blood flow calculations from the ASL scans were generated at each voxel and intensities were overlaid on a T1-weighted anatomical scan of the eye, which is seen in Figure 3. Furthermore, these images were analyzed alongside fluorescein angiography images and OCT measurements of the choroid. Blood flow results were taken as an average across all voxels (the blood flow map) along the ROI at the full thickness of the choroid and retina, which are summarized in Table 2, as well as results of the subjects' fluorescein angiography and choroidal thickness measurements.

The participants all presented with differing ocular conditions, and as there were too many variables between participants, it did not deem appropriate to average the results across all of them. Thus, results are analyzed on a subject-by-subject basis, whereby ASL results are compared between the two eyes, as well as their OCT and fluorescein angiography results.

Discussion

Our pilot study demonstrated that the MRI in ASL mode could be a feasible non-invasive tool for assessing the chorioretinal blood flow and hence revealing localized normal and compromised ocular perfusion in individuals. For normal healthy individuals, previous ASL studies have demonstrated that averaged values of chorioretinal perfusion at the posterior pole across the full thickness of the retina and choroid decrease with increasing age [28]. Individuals aged between 24 and 36 years were found to have an average peak blood flow of 270 ± 98 mL/100 mL/min, and those aged between 37 and 68 years were found to have an average peak blood flow of 161 ± 54 mL/100 mL/min [28]. This is consistent with prior studies, which have found a similar posterior pole chorioretinal perfusion of 149 ±48 mL/100 mL/min [24]. In comparison, despite the heterogeneous mix of ocular conditions present in this pilot study, with each participant exhibiting different choroidal thicknesses and arterial filling rates, all recorded significantly reduced perfusion on ASL. For example, whilst participant 2 had significantly delayed arterial filling and a normal choroidal thickness, participant 1 had normal arterial filling but very thin choroids, and yet both recorded reduced chorioretinal perfusion.

Arterial filling time is the time taken for the branches of the central retinal artery to be filled with auto-fluorescent sodium fluorescein, using dynamic high-speed fluorescein angiography. In healthy individuals with a normal chorioretinal vasculature, the arterial filling time is 2.69 ± 1.25 s [29, 30], but in practice a value of less than 4 s is considered normal. The arterial filling time is assumed to be indicative of chorioretinal perfusion, as arterial filling time and blood flow are presumed to be inversely proportional [29], with an increased arte-

rial filling time suggesting an obstruction or an increase in resistance to blood flow within the arterial tree proximal to the globe. However, without information about vessel diameters or total volume in the vascular bed, a direct relationship between arterial filling time and ocular perfusion cannot be established [31]. Nevertheless, studies have documented a delayed arterial filling time in participants suffering from central retinal artery occlusion, ocular ischemic syndrome, and diabetic retinopathy [32–35]. Participants 2 and 3 in our study had significantly delayed arterial filling times and these findings were in keeping with their severe ocular ischemic syndrome as manifest clinically; namely critically compromised central retinal filling pressures, the presence of confluent mid-peripheral retinal blot hemorrhages, significant retinal capillary non-perfusion on angiography, and clinically significant carotid stenosis (>90%). In contrast, participants 1 and 4 had normal arterial filing times on dynamic angiography and normal retinal capillary filling, observations which were in keeping with the clinical findings. However, in all 4 individuals the chorioretinal perfusion as measured by ASL was significantly reduced, and curiously the patient with the most profound ocular ischemia clinically recorded the highest perfusion rate, although still significantly reduced compared to controls. Where one might have expected to observe reduced chorioretinal perfusion in the 2 participants with ocular ischemic syndrome, our finding that the chorioretinal perfusion of the 2 participants with normal arterial filling times on angiography was also significantly reduced invites further explanation.

Although a long established clinical tool, dynamic fluorescein angiography is an imperfect investigation. The assumption that a delayed arterial transit is synonymous with reduced oxygen delivery to the target tissues may not be correct, and in contrast, a normal arterial filling does not mean that the tissue oxygenation is normal as it tells one nothing about the volume of blood delivered to these target tissues. As such, a delayed arterial filling time is not in itself diagnostic for tissue ischemia. However, in the context of the clinical and angiographic findings of severe ocular ischemic syndrome, we are confident that the angiographic findings in participants 2 and 3 do represent the presence of a significantly compromised arterial tree proximal to the globe and hence reduced tissue perfusion in these eyes. Similarly, we are confident that the lack of clinical signs of *global* retinal ischemia in cases 1 and 4 are indicative of a normal proximal arterial tree in these individuals. Our interpretation of the results of the dynamic and static angiography conducted on our 4 participants is as follows:

1. In participants 2 and 3, significant tissue ischemia was present as a consequence of a clinically critical obstruction in the arterial tree proximal to the globe: in both cases within the carotid arteries.
2. In participants 1 and 4, there was no such obstruction and as a result the arterial filling times were normal. As such, an alternative explanation is required for the significantly reduced perfusion that was observed on MRI ASL in participants1 and 4.

Aside from the rate of blood flow, the other factor that will influence perfusion of the posterior pole in ASL is the volume of the vascular tissue under test. Whilst a direct volumetric analysis of the chorioretinal vascular tissues was not performed in this study, we did measure a surrogate marker, namely central macular thickness as measured by EDI OCT. Although central macular choroidal thickness is known to decrease with increasing age, excessive choroidal thinning is also observed in AMD and pathological myopia [36]. In healthy subjects, the average central macular thickness of the retina and choroid are 209.1 ± 12.9 μm

and 292.7 ± 77.3 μm, respectively [2]. With a choroidal thickness of just 25 μm (OD) and 27 μm (OS) in participant 1 and 46 μm (OD) and 76 μm (OS) in participant 4, they had a very attenuated choroidal thickness former due to pathological myopia, and latter due to dry AMD. The observation that the 2 participants with thinned choroids but normal dynamic and static angiographic findings also recorded significantly reduced chorioretinal perfusion on ASL may offer a useful insight into the relative contribution of blood flow rate and vascular tissue volume to the results obtained from ASL.

Perfusion as measured by ASL is a function of blood flow and the tissue volume. As such, patients with very thin choroids, and hence reduced vascular volume, would be expected to have a reduced perfusion on ASL, irrespective of the findings on angiography, as was observed in this study. Moreover, participants who had near normal choroidal thicknesses but a critically reduced perfusion pressure (and hence blood flow rate, caused by a severe stenosis within the proximal arterial tree) also recorded a low perfusion figure on ASL, attesting to the sensitivity of our technique to accurately measure chorioretinal perfusion. Overall, this pilot study suggests that both arterial filling rate (perfusion pressure) and choroidal thickness (anatomy) have a role in determining the perfusion of the posterior pole as measured by ASL. However, the fact that participant 1 had both the thinnest choroid and the most compromised perfusion as measured by ASL is intriguing and, if repeatable, may suggest that choroidal thickness is more important in determining chorioretinal perfusion on ASL than arterial filling times as measured on dynamic fluorescein angiography.

Despite the undoubted success of anti-VEGF treatments in treating the neovascular component of the disease, advanced AMD remains the leading cause of blindness in industrialized nations. Both advanced AMD and pathological myopia are associated with progressive atrophy of the retinal pigment epithelium and choroidal neovascularization, and the extent of both these processes, at least for AMD, are inversely correlated with choroidal thickness [2, 36–39]. At present, the role that thinning of the choroid, and the choriocapillaris in particular, play in the pathophysiology of AMD and myopic macular degeneration remains a matter of debate and currently we lack a reliable, non-invasive, quantitative tool for accurately measuring localized chorioretinal blood flow and perfusion.

Prior to any intervention studies that might utilize ASL as a perfusion measurement technology, it is essential to separate the retinal and choroidal contributions of the ocular perfusion. We are actively working towards such improved implementation of the ASL pulse sequence, optimized for differentiating the retinal and choroidal circulations, but multiple technical challenges remain.

The data we present in this pilot study represent for the first time that MRI ASL has been used to investigate eyes of individuals who have ocular pathology leading to reduced perfusion within the chorioretinal circulation. We believe that our technique will fill this gap in our armory of investigative tools and thus has the potential to advance our understanding of the pathophysiology of ischemia and neovascularization of the posterior pole.

Future Directions

We are currently designing a large-scale MRI ASL study, whereby allowing for comparison between individuals diagnosed with chorioretinal ischemia due to AMD. Thus, we may

better understand how each of the factors of the differing conditions (i.e., arterial filling time or choroidal thickness) will affect the chorioretinal blood flow. Although MRI is certainly not a cheap technology, it has become ever more common and accessible over the last decade. The current cost of our ASL MRI scan (in the country of the authors) is less than that of 1 intravitreal injection of anti-VEGF agent for the treatment of wet AMD. Due to the often slow progression rate of dry AMD, we believe that in the future, an annual ASL MRI scan of these patients is sufficient for establishing the baseline and then monitoring the progression of the disease. For faster evolving pathologies such as diabetic maculopathy, a more frequent (twice a year) scanning protocol may be frequent enough. While, this frequency of scans is affordable in developed countries, it will take some time to become accessible in the developing world.

Acknowledgements

The researchers wish to thank the clinical radiologists at the Centre for Advanced MRI (University of Auckland) for performing the scans. They also wish to thank Miss Pavani Kurra for her role in recruitment of patients.

This research was funded by a Health Research Council of New Zealand Award (project #3705378).

Statement of Ethics

This study was approved by the University of Auckland Human Participants Ethics Committee.

Disclosure Statement

This work has never been presented elsewhere. The authors have no proprietary interests in the materials described in the article.

References

1 Field GD, Chichilnisky EJ: Information processing in the primate retina: circuitry and coding. Annu Rev Neurosci 2007;30:1–30.

2 Ikuno Y, et al: Reproducibility of retinal and choroidal thickness measurements in enhanced depth imaging and high-penetration optical coherence tomography. Invest Ophthalmol Vis Sci 2011;52:5536–5540.

3 Maleki N, et al: The effect of hypercarbia and hyperoxia on the total blood flow to the retina as assessed by magnetic resonance imaging. Invest Ophthalmol Vis Sci 2011;52:6867–6874.

4 Erdem CZ, et al: Doppler measurement of blood flow velocities in extraocular orbital vessels in patients with obstructive sleep apnea syndrome. J Clin Ultrasound 2003;31:250–257.

5 Bek T: Inner retinal ischaemia: current understanding and needs for further investigations. Acta Ophthalmol 2009;87:362–367.

6 Terelak-Borys B, Skonieczna K, Grabska-Liberek I: Ocular ischemic syndrome – a systematic review. Medical Science Monitor 2012;18:RA138–RA144.
7 Friedman E, Smith TR, Kuwabara T: Retinal microcirculation in vivo. Invest Ophthalmol 1964;3:217–226.
8 Campochiaro PA: Molecular pathogenesis of retinal and choroidal vascular diseases. Prog Retin Eye Res 2015;49:67–81.
9 Kermorvant-Duchemin E, et al: Understanding ischemic retinopathies: emerging concepts from oxygen-induced retinopathy. Doc Ophthalmol 2010;120:51–60.
10 Dugan JD, Green WR: Ophthalmologic manifestations of carotid occlusive disease. Eye 1991;5:226–238.
11 Malhotra R, Gregory-Evans K: Management of ocular ischaemic syndrome. Br J Ophthalmol 2000;84:1428–1431.
12 Peng Q, et al: MRI of blood flow of the human retina. Magn Reson Med 2011;65:1768–1775.
13 Hassenstein A, Meyer CH: Clinical use and research applications of Heidelberg retinal angiography and spectral-domain optical coherence tomography – a review. Clin Exp Ophthalmol 2009;37:130–143.
14 Axer-Siegel R, et al: Angiographic and flow patterns of retinal choroidal anastomoses in age-related macular degeneration with occult choroidal neovascularization. Ophthalmology 2002;109:1726–1736.
15 Choi W, et al: Choriocapillaris and choroidal microvasculature imaging with ultrahigh speed OCT angiography. PLoS One 2013;8:e81499.
16 Novotny HR, Alvis D: A method of photographing fluorescence in circulating blood of the human eye. Tech Doc Rep SAMTDR USAF Sch Aerosp Med 1960;60–82:1–4.
17 Staurenghi G, Flower RW: Clinical observations supporting a theoretical model of choriocapillaris blood flow in treatment of choroidal neovascularization associated with age-related macular degeneration. Am J Ophthalmol 2002;133:801–808.
18 Matsunaga D, et al: OCT angiography in healthy human subjects. Ophthalmic Surg Lasers Imaging Retina 2014;45:510–515.
19 Jia Y, et al: Quantitative optical coherence tomography angiography of choroidal neovascularization in age-related macular degeneration. Ophthalmology 2014;121:1435–1444.
20 Vaghefi E, Pontre B: Application of arterial spin labelling in the assessment of ocular tissues. Biomed Res Int 2016;2016:6240504.
21 Detre JA, et al: Applications of arterial spin labeled MRI in the brain. J Magn Reson Imaging 2012;35:1026–1037.
22 Alsop DC, et al: Recommended implementation of arterial spin-labeled perfusion MRI for clinical applications: a consensus of the ISMRM perfusion study group and the European consortium for ASL in dementia. Magn Reson Med 2015;73:102–116.
23 Wong EC: An introduction to ASL labeling techniques. J Magn Reson Imaging 2014;40:1–10.
24 Zhang Y, et al: Blood flow MRI of the human retina/choroid during rest and isometric exercise. Invest Ophthalmol Vis Sci 2012;53:4299–4305.
25 Maleki N, Dai W, Alsop DC: Blood flow quantification of the human retina with MRI. NMR Biomed 2011;24:104–111.
26 Penny WD, et al: Statistical Parametric Mapping: The Analysis of Functional Brain Images. Academic Press, 2011.
27 Wang J, et al: Arterial transit time imaging with flow encoding arterial spin tagging (FEAST). Magn Reson Med 2003;50:599–607.
28 Zhang Y, et al: Decreased retinal–choroidal blood flow in retinitis pigmentosa as measured by MRI. Doc Ophthalmol 2013;126:187–197.
29 Williamson TH: What is the use of ocular blood flow measurement? Br J Ophthalmol 1994;78:326.
30 Koyama T, et al: Retinal circulation times in quantitative fluorescein angiography. Graefes Arch Clin Exp Ophthalmol 1990;228:442–446.
31 Cioffi GA, Alm A: Measurement of ocular blood flow. J Glaucoma 2001;10(5 suppl 1):S62–S64.
32 Giuffre G: Delayed filling of retinal and ciliary circulation after central retinal artery occlusion. Doc Ophthalmol 1988;69:325–330.
33 Brown GC, Brown MM, Magargal LE: The ocular ischemic syndrome and neovascularization. Trans Pa Acad Ophthalmol Otolaryngol 1986;38:302–306.
34 Brown GC, Magargal LE: The ocular ischemic syndrome. Clinical, fluorescein angiographic and carotid angiographic features. Int Ophthalmol 1988;11:239–251.
35 Hwang JM, et al: Bilateral ocular ischemic syndrome secondary to giant cell arteritis progressing despite corticosteroid treatment. Am J Ophthalmol 1999;127:102–104.

36 Viola F, et al: Choroidal findings in dome-shaped macula in highly myopic eyes: a longitudinal study. Am J Ophthalmol 2015;159:44–52.

37 Chirco KR, et al: Structural and molecular changes in the aging choroid: implications for age-related macular degeneration. Eye (Lond) 2017;31:10–25.

38 Fujiwara T, et al: Enhanced depth imaging optical coherence tomography of the choroid in highly myopic eyes. Am J Ophthalmol 2009;148:445–450.

39 Sarks S: Ageing and degeneration in the macular region: a clinico-pathological study. Br J Ophthalmol 1976;60:324–341.

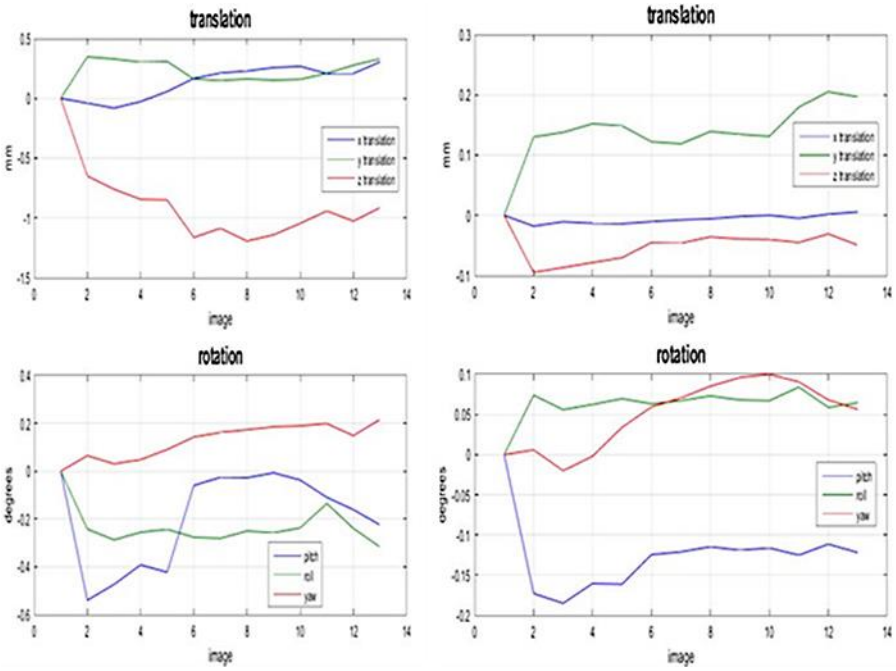

Fig. 1. Six estimated parameters (3 translations + 3 rotations) of rigid body transformation before (left) and after (right) the realignment process. Both translational and rotational differences between the reference images and each time course image were reduced and far below the image resolution (0.8 mm).

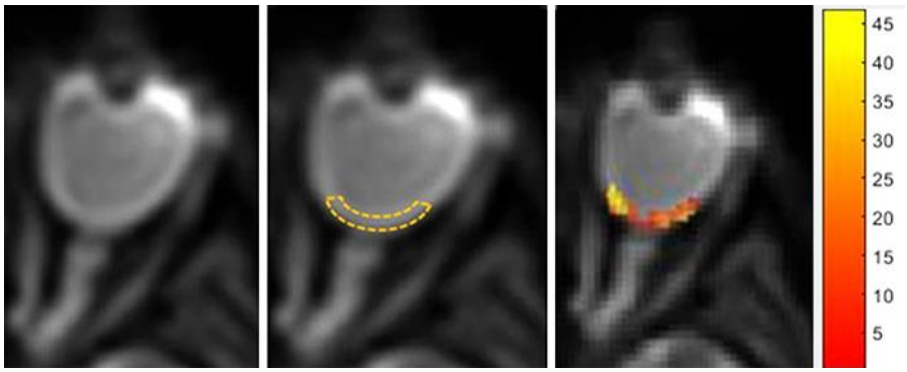

Fig. 2. The slice image that contained distinct optical nerves and other orbital tissues was selected for each participant (left). A customized mask was drawn on the region of the retina/choroidal complex (middle). The pixel-wise blood flow maps overlay on the reference M0 image (right). The color bar is in the unit of mL/100 g/min.

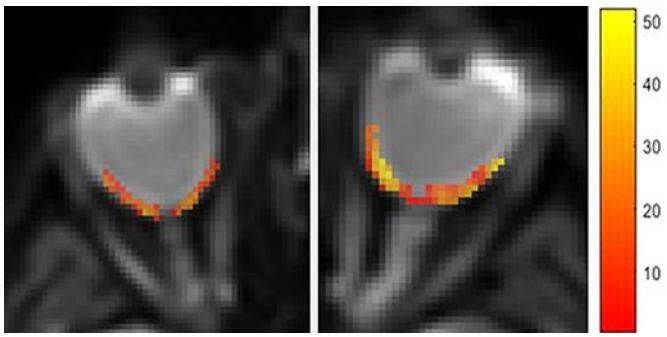

Fig. 3. The anatomical MR image of both eyes of participant 4, superimposed with ASL perfusion signal (mL/100 g/min). The perfusion signal is markedly larger around the optic nerve head and decreases towards the periphery of the retina.

Table 1. Participants' information

Participant	Age, years	Ocular diagnosis	Choroidal thickness, μm	Arterial filling time, s
1	56	pathological myopia (OU)	25 (OD) 27 (OS)	4 (OD) Not known (OS)
2	67	ocular ischemic syndrome (OU)	225 (OD) 267 (OS)	19 (OD) 16 (OS)
3	83	ocular ischemic syndrome (OU)	105 (OD) 113 (OS)	17 (OD) Not known (OS)
4	69	Dry AMD (OU)	46 (OD) 76 (OS)	4 (OD) Not known (OS)

Table 2. Summary of ASL perfusion signal for all 4 participants

Participant	Eye	Blood flow as measured by ASL, mL/100 mg/min	Arterial filling time as measured by fluorescein angiography, s	Choroidal thickness as measured by EDI OCT, μm
1	OD OS	17.17 15.28	<4 Not known	25 27
2	OD OS	43.00 27.19	19 16	225 267
3	OD OS	19.39 27.54	17 Not known	105 113
4	OD OS	20.54 21.82	<4 Not known	46 76